

A general class of surrogate functions for stable and efficient reinforcement learning

Sharan Vaswani^{1*}Olivier Bachem²Simone Totaro³Robert Müller⁴Shivam Garg⁵Matthieu Geist²Marlos C. Machado^{5,6}Pablo Samuel Castro²Nicolas Le Roux^{3,7*}¹Simon Fraser University²Google Brain³Mila, Université de Montréal⁴TU Munich⁵Amii, University of Alberta⁶DeepMind⁷Microsoft Research

Abstract

Common policy gradient methods rely on the maximization of a sequence of surrogate functions. In recent years, many such surrogate functions have been proposed, most without strong theoretical guarantees, leading to algorithms such as TRPO, PPO or MPO. Rather than design yet another surrogate function, we instead propose a general framework (FMA-PG) based on functional mirror ascent that gives rise to an entire family of surrogate functions. We construct surrogate functions that enable policy improvement guarantees, a property not shared by most existing surrogate functions. Crucially, these guarantees hold regardless of the choice of policy parameterization. Moreover, a particular instantiation of FMA-PG recovers important implementation heuristics (e.g., using forward vs reverse KL divergence) resulting in a variant of TRPO with additional desirable properties. Via experiments on simple bandit problems, we evaluate the algorithms instantiated by FMA-PG. The proposed framework also suggests an improved variant of PPO, whose robustness and efficiency we empirically demonstrate on the MuJoCo suite.

1 Introduction

Policy gradient (PG) methods (Williams, 1992; Sutton et al., 2000; Konda and Tsitsiklis, 2000; Kakade, 2002) are an important class of model-free methods in reinforcement learning. They enable a differentiable policy parameterization and can easily handle function approximation and structured state-action spaces. PG methods based on REINFORCE (Williams and Peng, 1991) are equipped with strong theoretical guarantees in restricted settings (Agarwal et al., 2020; Mei et al., 2020; Cen et al., 2020). For these methods, each policy update requires recomputing the policy gradient. This in turn requires interacting with the environment or the simulator which can be computationally expensive.

On the other hand, methods such as TRPO (Schulman et al., 2015), PPO (Schulman et al., 2017) and MPO (Abdolmaleki et al., 2018) support off-policy updates, i.e. they can update the policy without requiring additional interactions with the environment. These methods are efficiently implementable and have good empirical performance (Dhariwal et al., 2017). All of these methods rely on constructing *surrogate functions* of the policy, then updating the policy by maximizing these surrogates. Unfortunately, most of these surrogate functions (including those for PPO, TRPO and MPO) do not have strong theoretical guarantees. Consequently, this class of PG methods only has performance guarantees in the tabular setting (Kakade and Langford, 2002; Schulman et al., 2015; Neu et al., 2017; Geist et al., 2019; Shani et al., 2020), and some of these can even fail to converge in simple scenarios (Hsu et al., 2020). More importantly, *there is no systematic way to design theoretically principled surrogate functions, or a unified framework to analyze their properties*. We ad-

*Work done while Sharan Vaswani was at Amii, University of Alberta. Correspondence to vaswani.sharan@gmail.com and nicolas.le.roux@gmail.com.

dress these issues through the following contributions.

Functional mirror ascent for policy gradient:

In Section 3, we construct surrogate functions using mirror ascent on a functional representation of the policy itself, rather than on its parameters. We call this approach functional mirror ascent (FMA) and derive its update for policy gradient methods. The FMA update results in a surrogate function that is independent of the policy parameterization. We use it to propose FMA-PG (FMA for PG), a general framework for constructing surrogate functions and introduce a generic policy optimization algorithm that relies on approximately maximizing a sequence of surrogate functions.

Theoretical guarantees for FMA-PG: In Section 4, we explain the theoretical advantages of using FMA-PG. In particular, we describe a sufficient condition that guarantees that maximizing the sequence of surrogate functions instantiated by FMA-PG will result in monotonic policy improvement and ensure convergence to a stationary point. Crucially, *these guarantees hold regardless of the choice of policy parameterization*.

Instantiating the FMA-PG framework: In Section 5, we instantiate the FMA-PG framework with two common functional representations – direct and softmax representations. For each of these, we compare the resulting surrogate function to existing methods in the literature. For each representation, we prove that a specific surrogate function instantiated by FMA-PG satisfies the sufficient condition in Section 4. Consequently, maximizing it guarantees monotonic policy improvement for *arbitrarily complicated policy parameterizations* including neural networks. Such a property is not shared by existing surrogate functions including those for PPO, TRPO and MPO.

For the softmax functional representation, FMA-PG results in a surrogate function that is a more stable variant of TRPO (Schulman et al., 2015) and MDPO (Tomar et al., 2020). Moreover, it recovers implementation heuristics (e.g. using forward vs reverse KL divergence) in a principled manner. Additionally, in Appendix A, we show that FMA-PG can handle stochastic value gradients (Heess et al., 2015).

Experimental evaluation: Finally, in Section 6, we evaluate the performance of surrogate functions instantiated by FMA-PG on simple bandit settings. FMA-PG also suggests a variant of PPO (Schulman et al., 2017), whose robustness and efficiency we demonstrate on continuous control tasks in the MuJoCo environment (Todorov et al., 2012).

2 Problem formulation

We consider an infinite-horizon discounted Markov decision process (MDP) (Puterman, 1994) defined by the

tuple $\mathcal{M} = \langle \mathcal{S}, \mathcal{A}, p, r, d_0, \gamma \rangle$ where \mathcal{S} is a potentially infinite set of states, \mathcal{A} a potentially infinite action set, $p : \mathcal{S} \times \mathcal{A} \rightarrow \Delta^{\mathcal{S}}$ the transition probability function, $r : \mathcal{S} \times \mathcal{A} \rightarrow \mathbb{R}$ the reward function, d_0 the initial distribution of states, and $\gamma \in [0, 1)$ the discount factor.

Each policy π induces a distribution $p^\pi(\cdot|s)$ over actions for each state s . It also induces a measure d^π over states such that $d^\pi(s) = \sum_{\tau=0}^{\infty} \gamma^\tau \mathbb{P}(s_\tau = s | s_0 \sim d_0, a_\tau \sim p^\pi(a_\tau|s_\tau))$. Similarly we define μ^π as the measure over state-action pairs induced by policy π , implying that $\mu^\pi(s, a) = d^\pi(s)p^\pi(a|s)$ and $d^\pi(s) = \sum_a \mu^\pi(s, a)$. The expected discounted return for π is defined as $J(\pi) = \mathbb{E}_{s_0, a_0, \dots} [\sum_{\tau=0}^{\infty} \gamma^\tau r(s_\tau, a_\tau)]$, where $s_0 \sim d_0, a_\tau \sim p^\pi(a_\tau|s_\tau)$, and $s_{\tau+1} \sim p(s_{\tau+1}|s_\tau, a_\tau)$. Given a class of feasible policies Π , the agent’s objective is to learn the policy that maximizes the expected discounted return. We denote by $\pi^* := \arg \max_{\pi \in \Pi} J(\pi)$ as the *optimal policy* in the class.

We call the set of distributions $p^\pi(\cdot|s)$ for each s or the measure d^π *functional representations* of the policy π . Note that a single policy π can have multiple functional representations. In general, optimizing J directly with respect to any functional representation of π is intractable. Consequently, the standard approach is to parameterize π by a set of parameters $\theta \in \mathbb{R}^d$ and to directly optimize J with respect to θ . However, it is critical to remember that *the functional representation of a policy is independent of its parameterization*.

There are other possible functional representations of a policy besides the two mentioned above. For example, since $p^\pi(\cdot|s)$ is a probability distribution, one can write $p^\pi(a|s) = \exp(z^\pi(a, s)) / \sum_{a'} \exp(z^\pi(a', s))$, and represent π as the set of $z^\pi(a, s)$ for each (a, s) pair. We call this particular functional representation the *softmax representation*, as opposed to the set of $p^\pi(a|s)$ which we call the *direct representation*. In the next section, we describe how to use the functional representation of a policy to derive a surrogate function. Although multiple functional representations can be equivalent in the class of policies they define, they result in different surrogate functions (Sections 5.1 and 5.2). Finally, we note that functional representations are not limited to stochastic policies and one can, for instance, represent a deterministic, stationary policy by specifying the state-action mapping for each state (Appendix A).

3 Functional mirror ascent for policy gradient

In the previous section, we defined the functional representation of a policy. However, as we mentioned, typically, one cannot optimize J with respect to these representations directly, in which case the policy π is

parameterized. While the functional representation defines a policy’s sufficient statistics, the *policy parameterization* specifies the practical realization of these statistics and defines the set Π of realizable (representable) policies. The parameterization is independent of the functional representation, is explicit and determined by a *model* with parameters θ . For example, we could represent a policy by its state-action occupancy measure and use a linear parameterization to realize this measure, implying $\mu^\pi(s, a|\theta) = \langle \theta, \phi(s, a) \rangle$, where θ is the parameter to be optimized and $\phi(s, a)$ are the known features providing information about the state-occupancy measures. Similarly, we could use a neural-network parameterization for the variables that define a policy in its softmax representation, rewriting $z^\pi(a, s) = z^\pi(a, s|\theta)$. In order to compare to existing methods (Agarwal et al., 2020; Mei et al., 2020), we also define a *tabular parameterization*. For a finite state-action MDP with S states and A actions, choosing a tabular parameterization with the softmax representation results in $\theta \in \mathbb{R}^{SA}$ such that $\forall s \in \mathcal{S}, a \in \mathcal{A}$, $z^\pi(a, s|\theta) = \theta_{s,a}$.

Next, we describe a form of mirror ascent to directly update a policy’s functional representation.

3.1 Functional mirror ascent update

To state the functional mirror ascent (FMA) update, we define a strictly convex, differentiable function ϕ as the mirror map. We denote by $D_\phi(\pi, \mu)$ the Bregman divergence associated with the mirror map ϕ between policies π and μ . Each iteration $t \in [T]$ of FMA consists of the update and projection steps (Bubeck, 2015): Eq. (1) computes the gradient $\nabla_\pi J(\pi_t)$ with respect to the policy’s functional representation and updates π_t to $\pi_{t+1/2}$ using a step-size η ; Eq. (2) computes the Bregman projection of $\pi_{t+1/2}$ onto the class of realizable policies, obtaining π_{t+1} .

$$\pi_{t+1/2} = (\nabla\phi)^{-1}(\nabla\phi(\pi_t) + \eta\nabla J(\pi_t)), \quad (1)$$

$$\pi_{t+1} = \arg \min_{\pi \in \Pi} D_\phi(\pi, \pi_{t+1/2}). \quad (2)$$

The above FMA updates can also be written as (c.f. Bubeck, 2015):

$$\pi_{t+1} = \arg \max_{\pi \in \Pi} \left[\langle \pi, \nabla_\pi J(\pi_t) \rangle - \frac{1}{\eta} D_\phi(\pi, \pi_t) \right]. \quad (3)$$

Note that the FMA update is solely in the functional space, and is specified by the choice of the functional representation and mirror map. The update requires solving a sub-problem to project the updated policy onto the set Π . Since the policy parameterization defines the set Π of realizable policies, it influences the difficulty of solving this projection sub-problem as well

as the final policy π_{t+1} . For simple policy parameterizations such as tabular or when using a linear model, the set Π is convex and the minimization in Eq. (3) can be done exactly. When using more complex policy parameterizations (e.g. deep neural network), the set of realizable policies Π can become arbitrarily complicated and non-convex, making the projection in Eq. (3) infeasible. The FMA-PG framework overcomes this issue as follows.

3.2 FMA-PG framework

We assume that Π consists of policies that are realizable by a model parameterized by $\theta \in \mathbb{R}^d$. Throughout the paper, we will use π to refer to a policy’s functional representation, whereas $\pi(\theta)$ will refer to the parametric realization of π . We do not impose any restriction on the parameterization and any generic model (e.g. neural network) can be used to parameterize π . The choice of the policy parameterization is implicit in the $\pi(\theta)$ notation. For the special case of the tabular parameterization, $\pi = \pi(\theta) = \theta$.

Solving Eq. (2) iteratively may be interpreted as finding a path that starts from $\pi_{t+1/2}$ and gradually gets closer to the set Π . In this view, an approximate solution would be a point along that path that is not in the set Π , and consequently not realizable by a vector θ . Another perspective is to interpret solving Eq. (2) as finding a path *within* Π that starts from π_t , the previous policy (already in Π), and gets closer to $\pi_{t+1/2}$ (potentially outside Π). Any point along such a path is within Π and is thus realizable.

In other words, we replace (2) with another problem with the same solution:

$$\arg \min_{\pi \in \Pi} D_\phi(\pi, \pi_{t+1/2}) = \arg \min_{\theta \in \mathbb{R}^d} D_\phi(\pi(\theta), \pi_{t+1/2}). \quad (4)$$

With this reparameterization, no projection is required and the update in Eq. (3) can be written as a parametric, unconstrained optimization problem. This is a critical property as it makes FMA-PG applicable to any policy parameterization.

In particular, if $\pi_t = \pi(\theta_t)$, $\theta_{t+1} \in \mathbb{R}^d$ is the solution to the RHS of Eq. (4) and $\pi_{t+1} = \pi(\theta_{t+1})$, then Eq. (3) can be written as the maximization of a *surrogate function*,

$$\begin{aligned} \theta_{t+1} &= \arg \max_{\theta \in \mathbb{R}^d} \ell_t^{\pi, \phi, \eta}(\theta) \quad \text{where,} \\ \ell_t^{\pi, \phi, \eta}(\theta) &:= J(\pi(\theta_t)) + \langle \pi(\theta) - \pi(\theta_t), \nabla_\pi J(\pi(\theta_t)) \rangle \\ &\quad - \frac{1}{\eta} D_\phi(\pi(\theta), \pi(\theta_t)). \end{aligned} \quad (5)$$

The surrogate function $\ell_t^{\pi, \phi, \eta}(\theta)$ is a function of θ , but

Algorithm 1: Generic algorithm for policy optimization

Input: π (choice of functional representation), θ_0 (initial policy parameterization), T (PG iterations), m (inner-loops), η (step-size for functional update), α (step-size for parametric update)

```

for  $t \leftarrow 0$  to  $T - 1$  do
  Compute gradient  $\nabla_{\pi} J(\pi_t)$  and form function
   $\ell_t^{\pi, \phi, \eta}(\theta)$  as in Eq. (5)
  Initialize inner-loop:  $\omega_0 = \theta_t$ 
  for  $k \leftarrow 0$  to  $m$  do
     $\omega_{k+1} = \omega_k + \alpha \nabla_{\omega} \ell_t^{\pi, \phi, \eta}(\omega_k)$ 
  end
   $\theta_{t+1} = \omega_m$ 
   $\pi_{t+1} = \pi(\theta_{t+1})$ 
end
Return  $\theta_T$ 

```

it is specified by the choice of the functional representation, the mirror map Φ , and the step-size η . Note that as compared to Eq. (3), in Eq. (5), we added terms independent of θ which do not change the arg max but will prove useful to prove guarantees in Section 4. We have thus used the FMA update in Eq. (3) to specify a family of surrogate functions that can be used with any policy parameterization. We refer to this general framework of constructing surrogates for policy gradient methods as FMA-PG.

The surrogate function in Eq. (5) is non-concave in general and can be maximized using a gradient-based algorithm. We will use m gradient steps with a step-size α to maximize $\ell_t^{\pi, \phi, \eta}(\theta)$. With this choice, we can now state a generic policy optimization algorithm (pseudo-code in Algorithm 1). We see that the surrogate function $\ell_t^{\pi, \phi, \eta}$ acts as a “guide” for the parametric updates in the inner loop, similar to the supervised learning method proposed by Johnson and Zhang (2020).

Next we explain the theoretical advantage of using surrogate functions instantiated by FMA-PG.

4 Theoretical guarantees for FMA-PG

Recall that the policy is updated through the (potentially approximate) maximization of Eq. (5). To guarantee that maximizing the surrogate function improves the resulting policy, i.e. $J(\pi_{t+1}) \geq J(\pi_t)$, a sufficient condition is to have $\ell_t(\theta) \leq J(\pi(\theta))$ for all θ .

Indeed, if ℓ_t is a uniform lower-bound on J , then,

$$\begin{aligned}
 J(\pi_{t+1}) &= J(\pi(\theta_{t+1})) \geq \ell_t(\theta_{t+1}) \\
 &\geq \ell_t(\theta_t) \quad (\text{By maximizing the surrogate function}) \\
 &= J(\pi(\theta_t)) = J(\pi_t) \quad (\text{From Eq. (5)})
 \end{aligned}$$

For stating a more practical condition that guarantees that the surrogate function is a uniform lower-bound on J , we prove the following proposition in Appendix B.

Proposition 1 (Guarantee on surrogate function). *The surrogate function $\ell_t^{\pi, \phi, \eta}$ is a lower bound of J if and only if $J + \frac{1}{\eta}\phi$ is a convex function of π .*

The above proposition shows that the desired property is guaranteed by selecting an appropriate value of η that only depends on properties of J and the mirror map Φ in the functional space. Once again, we emphasize that the guarantees offered by the surrogate function are *independent of the parameterization*.

We have seen that if the surrogate is a uniform lower bound on J , then the equality of the two functions at $\theta = \theta_t$ (from Eq. (5)) guarantees that any improvement of the surrogate leads to an improvement of J . The following result states that improvement in the surrogate can be guaranteed provided that the parametric step-size α is chosen according to the smoothness of the surrogate function.

Theorem 1 (Guaranteed policy improvement for Algorithm 1). *Assume that ℓ_t is β -smooth w.r.t. the Euclidean norm and that η satisfies the condition of Proposition 1. Then, for any $\alpha \leq 1/\beta$, iteration t of Algorithm 1 guarantees $J(\pi_{t+1}) \geq J(\pi_t)$ for any number m of inner-loop updates.*

Note that Algorithm 1 and the corresponding theorem can be easily extended to handle stochastic parametric updates. This will guarantee that $\mathbb{E}[J(\pi_{t+1})] \geq J(\pi_t)$ where the expectation is over the sampling in the parametric SGD steps. Similarly, both the algorithm and theoretical guarantee can be generalized to incorporate the relative smoothness of $\ell_t(\theta)$ w.r.t. a general Bregman divergence (Lu et al., 2018).

For rewards in $[0, 1]$, $J(\pi)$ is upper-bounded by $\frac{1}{1-\gamma}$, and hence monotonic improvements to the policy guarantee convergence to a stationary point. We emphasize that the above result holds for *any arbitrarily complicated policy parameterization*. Hence, a successful PG method (one that reliably improves the policy) relies on appropriately setting two step-sizes: η at the functional level and α at the parametric level.

5 Instantiating FMA-PG

We now instantiate the FMA-PG framework with two common functional representations: the direct representation (Section 5.1) and the softmax representation (Section 5.2), deriving values for η for each.

5.1 Direct functional representation

In the direct functional representation, the policy π is represented by the set of distributions $p^\pi(\cdot|s)$ over actions for each state $s \in \mathcal{S}$. Using the policy gradient theorem (Sutton and Barto, 2018), in this case, $\frac{\partial J(\pi)}{\partial p^\pi(a|s)} = d^\pi(s)Q^\pi(s, a)$. Since $p^\pi(\cdot|s)$ is a set of distributions (one for each state), we define the mirror map as $\phi(\pi) = \sum_{s \in \mathcal{S}} w(s) \phi(p^\pi(\cdot|s))$, where $w(s)$ is a positive weighting on the states s . Note that the positive weights ensure that ϕ is a valid mirror-map. The resulting Bregman divergence is $D_\phi(\pi, \pi') = \sum_s w(s) D_\phi(p^\pi(\cdot|s), p^{\pi'}(\cdot|s))$, that is, the weighted sum of the Bregman divergences between the action distributions in state s . By choosing $w(s)$ equal to $d^{\pi_t}(s)$, and parameterizing the functional representation, i.e. $p^{\pi_t}(\cdot|s) = p^\pi(\cdot|s, \theta_t)$, we obtain the following form of the surrogate function:

$$\ell_t^{\pi, \phi, \eta}(\theta) = \mathbb{E}_{(s, a) \sim \mu^{\pi_t}} \left[\left(Q^{\pi_t}(s, a) \frac{p^\pi(a|s, \theta)}{p^\pi(a|s, \theta_t)} \right) - \frac{1}{\eta} D_\phi(p^\pi(\cdot|s, \theta), p^\pi(\cdot|s, \theta_t)) \right], \quad (6)$$

where the constants independent of θ were omitted. By choosing ϕ and η , the above surrogate function can be used with Algorithm 1. We now discuss how to set η that guarantees monotonic policy improvement when using the above surrogate function with the negative entropy mirror map, i.e. $\phi_{NE}(p^\pi(\cdot|s)) = -\sum_a p^\pi(a|s) \log p^\pi(a|s)$.

Proposition 2 (Improvement guarantees for direct functional representation). *Assuming that the rewards are in $[0, 1]$, when using the surrogate function in Eq. (6) with the mirror map chosen to be the negative entropy, then $J \geq \ell_t^{\pi, \phi, \eta}$ for $\eta \leq \frac{(1-\gamma)^3}{2\gamma|A|}$.*

This proposition is proved in Appendix C. In conjunction with the argument in Section 4, we can infer that using the direct functional representation with the negative entropy mirror map and $\eta \leq \frac{(1-\gamma)^3}{2\gamma|A|}$ ensures monotonic policy improvement for any policy parameterization.

Next, we discuss how the surrogate function in Eq. (6) and the resulting algorithm is related to existing methods. When using a tabular parameterization, i.e. when $\pi(\theta) = \theta$, we make the following connections:

Connection to uniform TRPO and MDPI: With the tabular parameterization, the proposed update is similar to the update in uniform TRPO (Shani et al., 2020) and Mirror Descent Modified Policy Iteration (Geist et al., 2019).

Connection to CPI: For finite states and actions, when using a tabular parameterization, the first term in Eq. (6) becomes the same as in conservative policy iteration (CPI) (Kakade and Langford, 2002). In CPI, the authors first derive the form $\sum_s d^\pi(s) \sum_a p^\pi(a|s) Q^{\pi_t}(s, a)$, then use a mixture policy to ensure that π is “close” to π_t and justify replacing $d^\pi(s)$ in the above expression by d^{π_t} . On the other hand, we use the FMA-PG framework to directly derive Eq. (6) and allow for the use of any Bregman divergence to ensure the proximity between π and π_t . While we derive the CPI update from an unconstrained optimization viewpoint, CPI has also been connected to constrained optimization with an equivalence to functional Frank-Wolfe (Scherrer and Geist, 2014).

Connection to REINFORCE-based methods: For finite states and actions, when using a tabular parameterization and Algorithm 1 with $m = 1$ (no off-policy updates), if we choose the (i) squared Euclidean distance as the mirror map, the proposed update is the same as standard REINFORCE (Williams and Peng, 1991; Agarwal et al., 2020) and (ii) negative entropy as the mirror map (implying that the resulting Bregman divergence is the KL divergence), the proposed update is equal to natural policy gradient (Kakade, 2001; Khodadadian et al., 2021).

Comparison to MDPO: With a direct functional representation, negative entropy as the mirror map and general policy parameterization, the resulting update is similar to the algorithm proposed in MDPO (Tomar et al., 2020). The difference between the two updates is that MDPO involves the advantage A^{π_t} instead of the Q^{π_t} term in Eq. (6).

However, the above formulation and MDPO have two main shortcomings. First, it involves $p^\pi(a|s, \theta)$, which means that for each parametric update, either (i) the actions need to be resampled on-policy, or (ii) the update involves an importance-sampling ratio $p^\pi(a|s, \theta)/p^\pi(a|s, \theta_t)$ like in Eq. (6). This requires clipping the ratio for stability, and can potentially result in overly conservative updates (Schulman et al., 2017). Moreover, with the mirror map as the negative entropy, the Bregman divergence is the reverse KL divergence, i.e. $D_\phi(p^\pi(\cdot|s, \theta), p^\pi(\cdot|s, \theta_t)) = \text{KL}(p^\pi(\cdot|s, \theta) || p^\pi(\cdot|s, \theta_t))$. The reverse KL divergence makes this objective *mode seeking*, in that the policy π might only capture a subset of the actions covered by π_t . Past works have addressed this issue either by adding entropy regu-

larization (Geist et al., 2019; Shani et al., 2020), or by simply reversing the KL, using the *forward* KL: $\text{KL}(p^\pi(\cdot|s, \theta_t) || p^\pi(\cdot|s, \theta))$ (Mei et al., 2019). However, using entropy regularization results in a biased policy, whereas the forward KL does not correspond to a valid Bregman divergence in p^π and can converge to a sub-optimal policy. We now show how FMA-PG with the softmax representation addresses both these issues in a principled way, providing a theoretical justification to heuristics that are used to improve PG methods.

5.2 Softmax functional representation

Since $p^\pi(\cdot|s)$ is a distribution, it has an equivalent softmax representation that we study in this section. The softmax functional representation results in the FMA update on the logits $z^\pi(a, s)$ of the conditional distributions $p^\pi(a|s)$. Formally, $p^\pi(a|s) = \frac{\exp(z^\pi(a, s))}{\sum_{a'} \exp(z^\pi(a', s))}$ and the policy gradient theorem yields $\frac{\partial J(\pi)}{\partial z^\pi(a, s)} = d^\pi(s) A^\pi(s, a) p^\pi(a|s)$. Here, $A^\pi(s, a)$ is the advantage function equal to $Q^\pi(s, a) - V^\pi(s)$. Similar to Section 5.1, we use a mirror map $\phi_z(z)$ that decomposes across states, i.e. $\phi_z(z) = \sum_s w(s) \phi_z(z^\pi(\cdot, s))$ for some positive weighting w . We denote the corresponding Bregman divergence as D_{ϕ_z} and choose $w(s) = d^{\pi_t}(s)$.

Parameterizing the logits as $z^\pi(a, s, \theta)$ and noting that $p^{\pi_t}(a|s) = p^\pi(a|s, \theta_t)$, we obtain the following form of the surrogate function:

$$\begin{aligned} \ell_t^{\pi, \phi, \eta}(\theta) &= E_{(s, a) \sim \mu^{\pi_t}} \left[A^{\pi_t}(s, a) p^\pi(a|s, \theta_t) \right. \\ &\quad \left. - \frac{1}{\eta} \sum_s w(s) D_{\phi_z}(z^\pi(\cdot, s, \theta), z^\pi(\cdot, s, \theta_t)) \right]. \end{aligned} \quad (7)$$

We now discuss how the surrogate function in Eq. (7) and the resulting algorithm relate to existing methods.

Connection to REINFORCE-based methods: For finite states and actions and when using a tabular parameterization and the squared Euclidean mirror map, Algorithm 1 with $m = 1$ leads to the same update as that of policy gradient with the softmax parameterization (Agarwal et al., 2020; Mei et al., 2020).

A more interesting surrogate emerges when ϕ is the *logsumexp*, i.e. $\phi_z(z) = \sum_s w(s) \log(\sum_a \exp(z^\pi(a, s)))$, and $w(s) = d^{\pi_t}(s)$. Then,

$$\ell_t^{\pi, \phi, \eta}(\theta) = E_{(s, a) \sim \mu^{\pi_t}} \left[\left(A^{\pi_t}(s, a) + \frac{1}{\eta} \right) \log \frac{p^\pi(a|s, \theta)}{p^\pi(a|s, \theta_t)} \right], \quad (8)$$

omitting the constant terms independent of θ . The full derivation of this computation can be found in Proposition 4 of Appendix C. We now discuss how to set η

that guarantees monotonic policy improvement when using the above surrogate function.

Proposition 3 (Improvement guarantees for softmax functional representation). *Assuming that the rewards are in $[0, 1]$, then the surrogate function in Eq. (8) satisfies $J \geq \ell_t^{\pi, \phi, \eta}$ for $\eta \leq 1 - \gamma$.*

This proposition is proved in Appendix C. As before, we can infer that using the softmax functional representation with the exponential mirror map and $\eta \leq 1 - \gamma$ ensures monotonic policy improvement for *any policy parameterization*. Although we have used the same η for all states s , the updates in Eqs. (6) and (8) can accommodate a different step-size $\eta(s)$ for each state. This is likely to yield tighter lower bounds and larger improvements in the inner loop. Determining such step-sizes is left for future work.

Unlike the formulation in Eq. (6), we see that Eq. (8) relies on the logarithm of the importance sampling ratios. Moreover, Eq. (8) can be written as

$$\begin{aligned} \ell_t^{\pi, \phi, \eta} &= \mathbb{E}_{s \sim d^{\pi_t}} \left[\mathbb{E}_{a \sim p^{\pi_t}} \left(A^{\pi_t}(s, a) \log \frac{p^\pi(a|s, \theta)}{p^\pi(a|s, \theta_t)} \right) \right. \\ &\quad \left. - \frac{1}{\eta} \text{KL}(p^\pi(\cdot|s, \theta_t) || p^\pi(\cdot|s, \theta)) \right]. \end{aligned} \quad (9)$$

Comparing to Eq. (6), we observe that the KL divergence is in the *forward* direction and is *mode covering*. This naturally prevents a mode-collapse of the policy and encourages exploration. We thus see that FMA-PG is able to recover an implementation heuristic (forward vs reverse KL) in a principled manner. Moreover, we can interpret Eq. (9) as a variant of TRPO with desirable properties, as we discuss next.

Comparison to TRPO: Comparing Eq. (9) to the TRPO update (Schulman et al., 2015), $\arg \max_{\theta \in \mathbb{R}^d} \mathbb{E}_{(s, a) \sim \mu^{\pi_t}} [A^{\pi_t}(s, a) \frac{p^\pi(a|s, \theta)}{p^\pi(a|s, \theta_t)}]$, such that $\mathbb{E}_{s \sim d^{\pi_t}} [\text{KL}(p^{\pi_t}(\cdot|s, \theta_t) || p^\pi(\cdot|s, \theta))] \leq \delta$, we observe that Eq. (9) involves the logarithm of p^π , which can be interpreted as a form of soft clipping due to the narrower range of the log ratio. Additionally, when the policy is modeled by a deep network with a final softmax layer, this leads to an objective concave in the last layer, which is in general easier to optimize than the original TRPO objective. Unlike TRPO, the proposed update enforces the proximity between policies via a regularization rather than a constraint. This modification has been recently found to be beneficial (Lazić et al., 2021). Finally, the parameter δ in TRPO is a hyper-parameter that needs to be tuned. In contrast, the regularization strength $1/\eta$ in proposed update can be determined theoretically (Proposition 3).

6 Experiments with the softmax functional representation

While this work focuses on providing a general framework for designing surrogate functions, we explore the behaviour of surrogates instantiated by the softmax functional representation in three different settings.

To avoid dealing with local maxima of J , we explore a multi-armed bandit, where we compare it to the exponential weights algorithm (EXP3) (Auer et al., 2002) in Section 6.1. The simplicity of the environment allows us to get a clearer understanding of the behaviour of each algorithm.

Finally, we tested the practical performance of FMA-PG using a larger-scale experiment on MuJoCo in Section 6.2. In addition to the increased complexity of the environments, this experiment allows us to explore how the surrogate behaves in the presence of a critic. Since the policies are parameterized as a deep network, the surrogate can only be maximized approximately.

6.1 Multi-armed bandit

For a stochastic multi-armed bandit problem, we compare EXP3, which corresponds to the single-state, tabular parameterization of FMA-PG with the direct representation and the negative entropy mirror map; to softmax EXP3 (*sEXP3*), which uses the softmax parameterization and the exponential mirror map. For EXP3, we use the standard importance weighting procedure (denoted as IWEXP3 in the plots) as well as the loss-based variation (Lattimore and Szepesvári, 2020) (denoted as LBIWEXP3). We swept over a range of step-sizes η , choosing the one which achieved the best average final regret for each algorithm over 50 runs (see Appendix D for details). Fig. 1 shows that *sEXP3* consistently achieves lower regret than both versions of EXP3, regardless of the number of arms (2, 10, 100) and the difficulty of the problem, as determined by the action gap.

6.2 Large-scale continuous control tasks

Since PPO (Schulman et al., 2017) requires clipping the importance sampling ratio, in order to make the resulting algorithm similar to PPO for ease of implementation, we included clipping with the surrogate function instantiated by FMA-PG. In particular, we modify Eq. (8) and the resulting surrogate given by:

$$\ell_t^{\pi, \phi, \eta}(\theta) = \mathbb{E}_{(s,a) \sim \mu^{\pi_t}} \left[A^{\pi_t}(s, a) \times \log \left(\text{clip} \left(\frac{p^\pi(a|s, \theta)}{p^\pi(a|s, \theta_t)}, \frac{1}{1 + \epsilon}, 1 + \epsilon \right) \right) \right],$$

We denote the above surrogate function and the resulting algorithm as *sPPO*. We investigate the performance of *sPPO* on five standard continuous control environments from the OpenAI Gym suite (Brockman et al., 2016): Hopper-v1, Walker2d-v1, HalfCheetah-v1, Ant-v1, and Humanoid-v1. As a baseline, we use the PPO implementation from Andrychowicz et al. (2021) with their standard configuration and all the hyperparameters set to their default values. We implement *sPPO* by adding a binary flag (`use_softmax`). We reemphasize that both algorithms use a critic and that the hyperparameters of the critic are tuned using PPO to avoid favoring our framework.

We investigate the differences between PPO and *sPPO* by training 180 different policies for each environment and all combinations of `use_softmax` $\in \{\text{True}, \text{False}\}$, $m \in \{10, 100\}$ and the importance weight capping value $\epsilon \in \{0.1, 0.3, 0.5, 0.7\}$ (a total compute of 1400 days with TPUv2). We evaluate each policy 18 times during training, using the action with largest probability rather than a sample. We compute the average return and 95% confidence intervals for each of the settings. The results are presented in Fig. 2, where we see that *sPPO* outperforms PPO across all environments. Furthermore, we see that the difference is more pronounced when the number of iterations m in the inner loop is increased (linestyles) or when less capping is used (columns). In Appendix E, we show additional results but with learning rate decay and gradient clipping disabled, two commonly used techniques to stabilize PPO training (Engstrom et al., 2019). In this setting, *sPPO* only suffers a mild degradation while PPO fails completely, again confirming the additional robustness of *sPPO* compared to PPO.

7 Conclusion

In this paper, we proposed FMA-PG, a general framework to design computationally efficient policy gradient methods. By disentangling the functional representation of a policy from its parameterization, we unified different PG perspectives, recovering several existing algorithms and implementation heuristics in a principled manner. FMA-PG enables the design of new, improved surrogate functions that lead to strong empirical results in various settings. By using the appropriate theoretically-determined hyper-parameters, FMA-PG guarantees policy improvement (and hence convergence to a stationary point) for the resulting PG method, even with arbitrarily complex policy parameterizations and for arbitrary number of inner-loop steps. We believe that our framework will further enable the systematic design of sample-efficient, off-policy PG methods.

Our theoretical results assume the exact computation

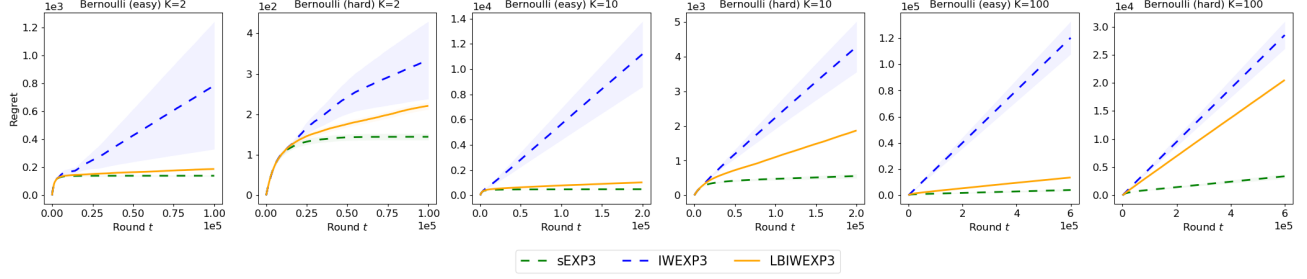


Figure 1: Comparing the average regret over 50 runs for two variants of EXP3 – with standard importance weights (IWEXP3) or loss-based importance weights (LBIWEXP3) to that of sEXP3. Both algorithms use a tuned step-size equal to 0.005. Shaded area represents two standard errors. We observe that sEXP3 consistently achieves lower regret. See Appendix D for more results.

of the action-value and advantage functions, and are thus limited in practice. In the future, we aim to handle sampling errors and extend these results to the actor-critic framework.

8 Acknowledgements

We would like to thank Veronica Chelu for suggesting the use of the log-sum-exp mirror map in Section 5. Nicolas Le Roux is funded by a CIFAR chair.

References

- Abdolmaleki, A., Springenberg, J. T., Tassa, Y., Munos, R., Heess, N., and Riedmiller, M. A. (2018). Maximum a posteriori policy optimisation. In *International Conference on Learning Representations (ICLR)*.
- Agarwal, A., Kakade, S. M., Lee, J. D., and Mahajan, G. (2020). Optimality and approximation with policy gradient methods in Markov decision processes. In *Conference on Learning Theory (COLT)*, pages 64–66.
- Andrychowicz, M., Raichuk, A., Stanczyk, P., Orsini, M., Girgin, S., Marinier, R., Hussenot, L., Geist, M., Pietquin, O., Michalski, M., et al. (2021). What matters for on-policy deep actor-critic methods? a largescale study. In *International conference on learning representations*.
- Auer, P., Cesa-Bianchi, N., Freund, Y., and Schapire, R. E. (2002). The nonstochastic multiarmed bandit problem. *SIAM journal on computing*, 32(1):48–77.
- Brockman, G., Cheung, V., Pettersson, L., Schneider, J., Schulman, J., Tang, J., and Zaremba, W. (2016). Openai gym. *arXiv preprint arXiv:1606.01540*.
- Bubeck, S. (2015). Convex optimization: Algorithms and complexity. *Foundations and Trends® in Machine Learning*, 8(3-4):231–357.
- Cen, S., Cheng, C., Chen, Y., Wei, Y., and Chi, Y. (2020). Fast global convergence of natural policy gradient methods with entropy regularization. *arXiv preprint arXiv:2007.06558*.
- Dhariwal, P., Hesse, C., Klimov, O., Nichol, A., Plappert, M., Radford, A., Schulman, J., Sidor, S., Wu, Y., and Zhokhov, P. (2017). Openai baselines. <https://github.com/openai/baselines>.
- Engstrom, L., Ilyas, A., Santurkar, S., Tsipras, D., Janoos, F., Rudolph, L., and Madry, A. (2019). Implementation matters in deep RL: A case study on PPO and TRPO. In *International conference on learning representations*.
- Geist, M., Scherrer, B., and Pietquin, O. (2019). A theory of regularized Markov decision processes. In *International Conference on Machine Learning*, pages 2160–2169. PMLR.
- Ghosh, D., C Machado, M., and Le Roux, N. (2020). An operator view of policy gradient methods. *Advances in Neural Information Processing Systems*, 33.
- Heess, N., Wayne, G., Silver, D., Lillicrap, T., Erez, T., and Tassa, Y. (2015). Learning continuous control policies by stochastic value gradients. In *Advances in Neural Information Processing Systems*, pages 2944–2952.
- Hsu, C. C.-Y., Mendler-Dünner, C., and Hardt, M. (2020). Revisiting design choices in proximal policy optimization. *arXiv preprint arXiv:2009.10897*.
- Johnson, R. and Zhang, T. (2020). Guided learning of nonconvex models through successive functional gradient optimization. In *International Conference on Machine Learning*, pages 4921–4930. PMLR.
- Kakade, S. (2001). A natural policy gradient. In *NIPS*, volume 14, pages 1531–1538.
- Kakade, S. and Langford, J. (2002). Approximately optimal approximate reinforcement learning. In *International Conference on Machine Learning (ICML)*, pages 267–274.

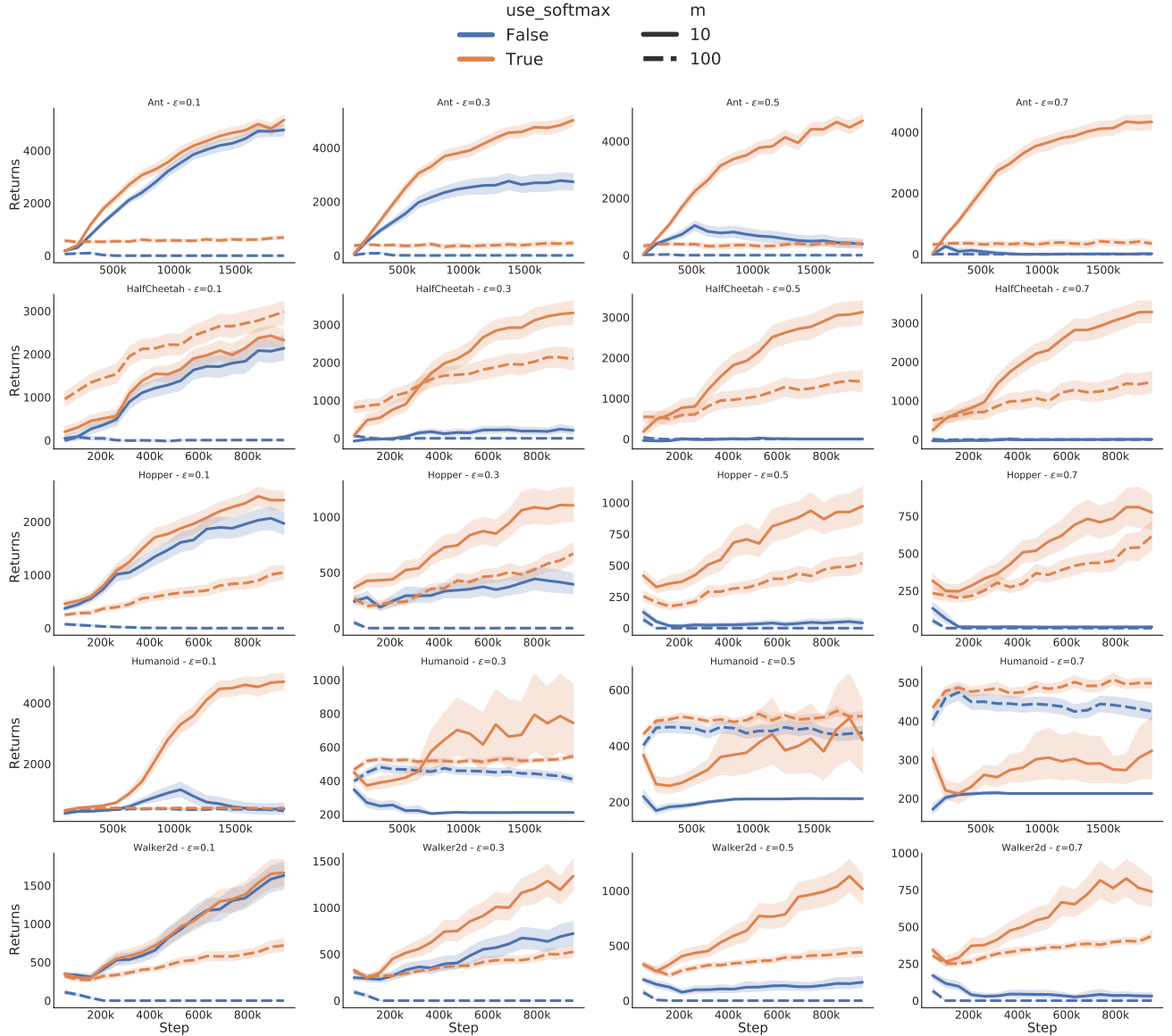


Figure 2: Average return and 95% confidence intervals (over 180 runs) for PPO and sPPO on 5 environments (rows) and for four different clipping values (columns). sPPO is more robust to large values of clipping, even more so when the number of updates in the inner loop grows (linestyle).

Kakade, S. M. (2002). A natural policy gradient. In *Advances in neural information processing systems*, pages 1531–1538.

Khodadadian, S., Jhunjhunwala, P. R., Varma, S. M., and Maguluri, S. T. (2021). On the linear convergence of natural policy gradient algorithm. *arXiv preprint arXiv:2105.01424*.

Konda, V. R. and Tsitsiklis, J. N. (2000). Actor-critic algorithms. In *Advances in neural information processing systems*, pages 1008–1014.

Lattimore, T. and Szepesvári, C. (2020). *Bandit algorithms*. Cambridge University Press.

Lazić, N., Hao, B., Abbasi-Yadkori, Y., Schuurmans, D., and Szepesvári, C. (2021). Optimization issues in kl-constrained approximate policy iteration. *arXiv preprint arXiv:2102.06234*.

Lu, H., Freund, R. M., and Nesterov, Y. (2018). Relatively smooth convex optimization by first-order methods, and applications. *SIAM Journal on Optimization*, 28(1):333–354.

Mei, J., Xiao, C., Huang, R., Schuurmans, D., and Müller, M. (2019). On principled entropy exploration in policy optimization. In *IJCAI*, pages 3130–3136.

Mei, J., Xiao, C., Szepesvári, C., and Schuurmans, D. (2020). On the global convergence rates of softmax

- policy gradient methods. In *International Conference on Machine Learning*, pages 6820–6829. PMLR.
- Neu, G., Jonsson, A., and Gómez, V. (2017). A unified view of entropy-regularized Markov decision processes. *CoRR*, abs/1705.07798.
- Puterman, M. L. (1994). *Markov Decision Processes: Discrete Stochastic Dynamic Programming*. John Wiley & Sons, Inc., USA.
- Scherrer, B. and Geist, M. (2014). Local policy search in a convex space and conservative policy iteration as boosted policy search. In *Joint European Conference on Machine Learning and Knowledge Discovery in Databases*, pages 35–50. Springer.
- Schulman, J., Levine, S., Abbeel, P., Jordan, M., and Moritz, P. (2015). Trust region policy optimization. In *International Conference on Machine Learning (ICML)*, pages 1889–1897.
- Schulman, J., Wolski, F., Dhariwal, P., Radford, A., and Klimov, O. (2017). Proximal policy optimization algorithms. *CoRR*, abs/1707.06347.
- Shani, L., Efroni, Y., and Mannor, S. (2020). Adaptive trust region policy optimization: Global convergence and faster rates for regularized mdps. In *Proceedings of the AAAI Conference on Artificial Intelligence*, volume 34, pages 5668–5675.
- Silver, D., Lever, G., Heess, N., Degris, T., Wierstra, D., and Riedmiller, M. (2014). Deterministic policy gradient algorithms. *Journal of Machine Learning Research*.
- Sutton, R. S. and Barto, A. G. (2018). *Reinforcement Learning: An Introduction*. MIT Press, 2 edition.
- Sutton, R. S., McAllester, D. A., Singh, S. P., and Mansour, Y. (2000). Policy gradient methods for reinforcement learning with function approximation. In *Advances in Neural Information Processing Systems (NeurIPS)*, pages 1057–1063.
- Todorov, E., Erez, T., and Tassa, Y. (2012). Mujoco: A physics engine for model-based control. In *2012 IEEE/RSJ International Conference on Intelligent Robots and Systems*, pages 5026–5033. IEEE.
- Tomar, M., Shani, L., Efroni, Y., and Ghavamzadeh, M. (2020). Mirror descent policy optimization. *arXiv preprint arXiv:2005.09814*.
- Vaswani, S., Mehrabian, A., Durand, A., and Kveton, B. (2020). Old dog learns new tricks: Randomized ucb for bandit problems.
- Williams, R. J. (1992). Simple statistical gradient-following algorithms for connectionist reinforcement learning. *Machine learning*, 8(3-4):229–256.
- Williams, R. J. and Peng, J. (1991). Function optimization using connectionist reinforcement learning algorithms. *Connection Science*, 3(3):241–268.

Supplementary material

Organization of the Appendix

- A Handling stochastic value gradients
- B Proofs for Section 4
- C Proofs for Section 5
- D Experimental details in the bandit setting
- E Additional experiments on MuJoCo environments

A Handling stochastic value gradients

Thus far we have worked with the original formulation of policy gradients where a policy is a distribution over actions given states. An alternative approach is that taken by stochastic value gradients (Heess et al., 2015), that rely on the reparametrization trick. In this case, a policy is not represented by a distribution over actions but rather by a set of actions. Formally, if ε are random variables drawn from a fixed distribution ν , then policy π is a deterministic map from $\mathcal{S} \times \nu \rightarrow \mathcal{A}$. This corresponds to the functional representation of the policy. The action a chosen by π in state s (when fixing the random variable $\epsilon = \varepsilon$) is represented as $\pi(s, \epsilon)$ and

$$J(\pi) = \sum_s d^\pi(s) \int_{\varepsilon} \nu(\varepsilon) r(s, \pi(s, \varepsilon)) d\varepsilon \quad (10)$$

and Silver et al. (2014) showed that $\frac{\partial J(\pi)}{\partial \pi(s, \epsilon)} = d^\pi(s) \nabla_a Q^\pi(s, a)|_{a=\pi(s, \epsilon)}$.

If the policy π is parameterized by model f with parameters θ , then $\pi(s, \epsilon) = f(\theta, s, \epsilon)$. If $f(\theta_t, \epsilon)$ and $f(\theta, \epsilon)$ are S -dimensional vectors, then Eq. (3) is given as

$$\theta_{t+1} = \arg \min \mathbb{E}_{\epsilon \sim \nu} \left[- \sum_s d^{\pi_t}(s) f(\theta, s, \epsilon) \nabla_a Q^{\pi_t}(s, a)|_{a=f(\theta_t, s, \epsilon)} + \frac{1}{\eta} D_\phi(f(\theta, \epsilon), f(\theta_t, \epsilon)) \right]. \quad (11)$$

Similar to Sections 5.1 and 5.2, we will use a mirror map that decomposes across states. Specifically, we choose $D_\phi(\pi, \mu) = \sum_{s \in \mathcal{S}} d^{\pi_t}(s) \|\pi(s) - \mu(s)\|^2$. With this choice, Eq. (11) can be written as:

$$\theta_{t+1} = \arg \max \left[\mathbb{E}_{s \sim d^{\pi_t}} \left[\mathbb{E}_{\epsilon \sim \nu} \left[f(\theta, s, \epsilon) \nabla_a Q^{\pi_t}(s, a)|_{a=f(\theta_t, s, \epsilon)} - \frac{1}{\eta} \|f(\theta, \epsilon) - f(\theta_t, \epsilon)\|^2 \right] \right] \right] \quad (12)$$

This formulation is similar to Eq (15) of (Silver et al., 2014), with Q^{π_t} instead of Q^π . Additionally, while the authors justified the off-policy approach with an approximation, our formulation offers guarantees provided η satisfies the condition of Proposition 1.

B Proofs for Section 4

Proposition 1 (Guarantee on surrogate function). *The surrogate function $\ell_t^{\pi, \phi, \eta}$ is a lower bound of J if and only if $J + \frac{1}{\eta} \phi$ is a convex function of π .*

Proof.

$$\begin{aligned}
 J(\pi) - \ell_t^{\pi, \phi, \eta}(\pi) &= J(\pi) - J(\pi_t) - \langle \pi - \pi_t, \nabla_{\pi} J(\pi_t) \rangle + \frac{1}{\eta} D_{\phi}(\pi, \pi_t) \\
 &= J(\pi) - J(\pi_t) - \langle \pi - \pi_t, \nabla_{\pi} J(\pi_t) \rangle + \frac{1}{\eta} (\phi(\pi) - \phi(\pi_t) - \langle \nabla_{\pi} \phi(\pi_t), \pi - \pi_t \rangle) \\
 &= \left(J + \frac{1}{\eta} \phi \right) (\pi) - \left(J + \frac{1}{\eta} \phi \right) (\pi_t) - \langle \pi - \pi_t, \nabla_{\pi} \left(J + \frac{1}{\eta} \phi \right) (\pi_t) \rangle.
 \end{aligned}$$

The last equation is positive for all π and all π_t if and only if $J + \frac{1}{\eta} \phi$ is convex. \square

Theorem 1 (Guaranteed policy improvement for Algorithm 1). *Assume that ℓ_t is β -smooth w.r.t. the Euclidean norm and that η satisfies the condition of Proposition 1. Then, for any $\alpha \leq 1/\beta$, iteration t of Algorithm 1 guarantees $J(\pi_{t+1}) \geq J(\pi_t)$ for any number m of inner-loop updates.*

Proof. Using the update in Algorithm 1 with $\alpha = \frac{1}{\beta}$ and the β -smoothness of $\ell_t(\omega)$, for all $k \in [m-1]$,

$$\ell_t(\omega_{k+1}) \geq \ell_t(\omega_k) + \frac{1}{2\beta} \|\nabla \ell_t(\omega_k)\|^2$$

After m steps,

$$\ell_t(\omega_m) \geq \ell_t(\omega_0) + \frac{1}{2\beta} \sum_{k=0}^{m-1} \|\nabla \ell_t(\omega_k)\|^2$$

Since $\theta_{t+1} = \omega_m$ and $\omega_0 = \theta_t$ in Algorithm 1,

$$\implies \ell_t(\theta_{t+1}) \geq \ell_t(\theta_t) + \frac{1}{2\beta} \|\nabla \ell_t(\theta_t)\|^2 + \sum_{k=1}^{m-1} \|\nabla \ell_t(\omega_k)\|^2$$

Note that $J(\pi_t) = \ell_t(\theta_t)$ and if η satisfies Proposition 1, then $J(\pi_{t+1}) \geq \ell_t(\theta_{t+1})$. Using these relations,

$$J(\pi_{t+1}) \geq J(\pi_t) + \underbrace{\frac{1}{2\beta} \|\nabla \ell_t(\theta_t)\|^2 + \sum_{k=1}^{m-1} \|\nabla \ell_t(\omega_k)\|^2}_{+ve} \implies J(\pi_{t+1}) \geq J(\pi_t).$$

\square

C Proofs for Section 5

In this section, we first prove the equivalence of the formulations in terms of the logits and in terms of $\log \pi$.

Lemma 1. *Let*

$$\phi(z) = \log \left(\sum_a \exp(z(a)) \right) \tag{13}$$

$$p^{\pi}(a) = \frac{\exp(z(a))}{\sum_{a'} \exp(z(a'))}. \tag{14}$$

Then

$$D_{\phi}(z, z') = KL(p^{\pi'} \| p^{\pi}). \tag{15}$$

where p^{π} and $p^{\pi'}$ use z and z' respectively.

Proof.

$$\begin{aligned}
 D_\phi(z, z') &= \log \left(\sum_a \exp(z(a)) \right) - \log \left(\sum_a \exp(z'(a)) \right) - \frac{\sum_a \exp(z'(a))(z(a) - z'(a))}{\sum_a \exp(z'(a))} \\
 &= \sum_a p^{\pi'}(a) \left(z(a) - z'(a) + \log \left(\sum_a \exp(z(a)) \right) - \log \left(\sum_a \exp(z'(a)) \right) \right) \\
 &= \sum_a p^{\pi'}(a) \log \frac{p^\pi(a)}{p^{\pi'}(a)}.
 \end{aligned}$$

□

Proposition 4.

$$\ell_t^{z^\pi, \phi, \eta}(\theta) = J(\pi_t) + E_{(s,a) \sim \mu^{\pi_t}} \left(A^{\pi_t}(s, a) + \frac{1}{\eta} \right) \log \frac{p^\pi(a|s, \theta)}{p^{\pi_t}(a|s, \theta)} \quad (16)$$

Proof. Because $\sum_a p^{\pi_t}(a|s) A^{\pi_t}(s, a) = 0$, we can shift all values of z by a term that does not depend on a without changing the sum, in particular by $\log(\sum_{a'} \exp(z^\pi(a', s|\theta)))$. Thus,

$$\begin{aligned}
 \ell_t^{z^\pi, \phi, \eta}(\theta) &= J(\pi_t) + E_{(s,a) \sim \mu^{\pi_t}} A^{\pi_t}(s, a) \left(z^\pi(a, s|\theta) - \log \left(\sum_{a'} \exp(z^\pi(a', s|\theta)) \right) \right) \\
 &\quad - \frac{1}{\eta} \sum_s d^{\pi_t}(s) D_{\phi_z}(z^\pi(\cdot, s|\theta), z^{\pi_t}(\cdot, s|\theta_t)) \\
 &= J(\pi_t) + E_{(s,a) \sim \mu^{\pi_t}} A^{\pi_t}(s, a) \log p^\pi(a|s, \theta) - \frac{1}{\eta} \sum_s d^{\pi_t}(s) D_{\phi_z}(z^\pi(\cdot, s|\theta), z^{\pi_t}(\cdot, s|\theta_t)) \\
 &= J(\pi_t) + E_{(s,a) \sim \mu^{\pi_t}} A^{\pi_t}(s, a) \log p^\pi(a|s, \theta) - \frac{1}{\eta} \sum_s d^{\pi_t}(s) KL((p^{\pi'}(\cdot|s) || p^\pi(\cdot|s))),
 \end{aligned}$$

where the last line is obtained using Lemma 1. Expanding the KL leads to the desired result. □

Proposition 2 (Improvement guarantees for direct functional representation). *Assuming that the rewards are in $[0, 1]$, when using the surrogate function in Eq. (6) with the mirror map chosen to be the negative entropy, then $J \geq \ell_t^{\pi, \phi, \eta}$ for $\eta \leq \frac{(1-\gamma)^3}{2\gamma|A|}$.*

Proof. Agarwal et al. (2020) show that, when using the direct parameterization, J is $\left(\frac{2\gamma|A|}{(1-\gamma)^3}\right)$ -smooth w.r.t. the Euclidean distance. By using the properties of relative smoothness (Lu et al., 2018), if the mirror map ϕ is μ -strongly convex w.r.t. Euclidean distance, then J is L -smooth with $L = (2\gamma|A|/(1-\gamma)^3\mu)$. Using the fact that negative entropy is 1-strongly convex w.r.t. the 1-norm, we can set $\eta = (1-\gamma)^3/2\gamma|A|$ in Eq. (6). □

To prove the value of η guaranteeing improvement for the softmax parameterization, we first need to extend a lower bound result from Ghosh et al. (2020):

Lemma 2. *Let us assume that the rewards are lower bounded by $-c$ for some $c \in \mathbb{R}$. Then we have*

$$J(\pi) \geq J(\pi_t) + E_{(s,a) \sim \mu^{\pi_t}} \left[\left(Q^{\pi_t}(s, a) + \frac{c}{1-\gamma} \right) \log \frac{p^\pi(a|s)}{p^{\pi_t}(a|s)} \right]. \quad (17)$$

Proof. Let us define the function J_ν for a policy ν as

$$J_\nu(\pi) = \sum_{h=0}^{+\infty} \gamma^h \int_{\tau_h} (r(s_h, a_h) + c) \left(1 + \log \frac{\pi_h(\tau_h)}{\nu_h(\tau_h)} \right) \nu_h(\tau_h) d\tau_h - \frac{c}{1-\gamma},$$

where τ_h is a trajectory of length h that is a prefix of a full trajectory τ and π_h is the policy restricted to trajectories of length h . We first show that it satisfies $J_\nu(\pi) \leq J(\pi)$ for any ν and any π such that the support of ν covers that of π .

Indeed, we can rewrite

$$\begin{aligned} J(\pi) &= \int_{\tau} \left(R(\tau) + \frac{c}{1-\gamma} \right) \pi(\tau) d\tau - \frac{c}{1-\gamma} \\ &= \int_{\tau} \left(\sum_h \gamma^h (r(a_h, s_h) + c) \right) \pi(\tau) d\tau - \frac{c}{1-\gamma} \quad (\text{using } \sum_h \gamma^h c = c/(1-\gamma)) \\ &= \sum_h \gamma^h \int_{\tau_h} (r(a_h, s_h) + c) \pi_h(\tau_h) d\tau_h - \frac{c}{1-\gamma}, \end{aligned}$$

where the last line is obtained by marginalizing over steps $h+1, \dots, +\infty$ for all h and all trajectories τ . Because $r(a_h, s_h) + c$ is positive, as the rewards are lower bounded by $-c$, we have

$$\begin{aligned} J(\pi) &= \sum_h \gamma^h \int_{\tau_h} (r(a_h, s_h) + c) \frac{\pi_h(\tau_h)}{\nu_h(\tau_h)} \nu_h(\tau_h) d\tau_h - \frac{c}{1-\gamma} \\ &\geq \sum_h \gamma^h \int_{\tau_h} (r(a_h, s_h) + c) \left(1 + \log \frac{\pi_h(\tau_h)}{\nu_h(\tau_h)} \right) \nu_h(\tau_h) d\tau_h - \frac{c}{1-\gamma} \quad (\text{using } x \geq 1 + \log x) \\ &= J_\nu(\pi). \end{aligned}$$

Let us denote J_ν^{SA} the right-hand side of Eq. (17), i.e.:

$$J_\nu^{SA}(\pi) = J(\nu) + E_{(s,a) \sim \mu^\nu} \left[\left(Q^\nu(s, a) + \frac{c}{1-\gamma} \right) \log \frac{p^\pi(a|s)}{p^\nu(a|s)} \right].$$

We now prove that J_ν has the same gradient as J_ν^{SA} :

$$\begin{aligned} \nabla_\theta J_\nu(\pi) &= \nabla_\theta \left(\sum_h \gamma^h \int_{\tau_h} (r(a_h, s_h) + c) \left(1 + \log \frac{\pi_h(\tau_h)}{\nu_h(\tau_h)} \right) \nu_h(\tau_h) d\tau_h \right) \\ &= \nabla_\theta \left(\sum_h \gamma^h \int_{\tau_h} (r(a_h, s_h) + c) \log \pi_h(\tau_h) \nu_h(\tau_h) d\tau_h \right) \\ &= \sum_h \gamma^h \int_{\tau_h} (r(a_h, s_h) + c) \nabla_\theta \log \pi_h(\tau_h) \nu_h(\tau_h) d\tau_h, \end{aligned}$$

where all terms independent of θ were moved outside of the gradient. As the log probability of a trajectory decomposes into a sum of the probabilities of actions given states and of the transition probabilities, and as the latter are independent of θ , we get

$$\begin{aligned} \nabla_\theta J_\nu(\pi) &= \sum_h \gamma^h \int_{\tau_h} (r(a_h, s_h) + c) \nabla_\theta \log \pi_h(\tau_h) \nu_h(\tau_h) d\tau_h \\ &= \sum_h \gamma^h \int_{\tau_h} (r(a_h, s_h) + c) \left(\sum_{h'} \nabla_\theta \log p^\pi(a_{h'}|s_{h'}) \right) \nu_h(\tau_h) d\tau_h \\ &= \int_{\tau} \sum_{h'} \nabla_\theta \log p^\pi(a_{h'}|s_{h'}) \left(\sum_{h=h'}^{+\infty} \gamma^h (r(a_h, s_h) + c) \right) \nu(\tau) d\tau. \end{aligned}$$

But

$$\begin{aligned} \sum_{h=h'}^{+\infty} \gamma^h (r(a_h, s_h) + c) &= \gamma^{h'} \left(Q^\nu(s, a) + \frac{c}{1-\gamma} \right) \\ \int_{\tau} \nu(\tau) d\tau 1_{a_{h'}=a} 1_{s_{h'}=s} &= d_\nu^{h'}(s) \nu(a|s), \end{aligned}$$

with $d_\nu^{h'}(s)$ the undiscounted probability of reaching state s at timestep h' . Hence, we have

$$\begin{aligned} \nabla_\theta J_\nu(\pi) &= \int_{\tau} \sum_{h'} \nabla_\theta \log p^\pi(a_{h'}|s_{h'}) \left(\sum_{h=h'}^{+\infty} \gamma^h (r(a_h, s_h) + c) \right) \nu(\tau) d\tau \\ &= \sum_{h'} \sum_s \sum_a \nabla_\theta \log p^\pi(a|s) d_\nu^{h'}(s) \nu(a|s) \gamma^{h'} \left(Q^\nu(s, a) + \frac{c}{1-\gamma} \right) \\ &= \sum_{h'} \gamma^{h'} \sum_s d_\nu^{h'}(s) \sum_a \nabla_\theta \log p^\pi(a|s) \nu(a|s) \left(Q^\nu(s, a) + \frac{c}{1-\gamma} \right) \\ &= \sum_s d^\nu(s) \sum_a \left(Q^\nu(s, a) + \frac{c}{1-\gamma} \right) \nu(a|s) \nabla_\theta \log p^\pi(a|s) \\ &= \nabla_\theta \left(\sum_s d^\nu(s) \sum_a \left(Q^\nu(s, a) + \frac{c}{1-\gamma} \right) \nu(a|s) \log p^\pi(a|s) \right) \\ &= \nabla_\theta \left(J(\nu) + E_{(s,a) \sim \mu^\nu} \left[\left(Q^\nu(s, a) + \frac{c}{1-\gamma} \right) \log \frac{p^\pi(a|s)}{p^\nu(a|s)} \right] \right) \\ &= \nabla_\theta J_\nu^{SA}(\pi), \end{aligned}$$

with $d^\nu(s)$ the unnormalized probability of s under the *discounted* stationary distribution.

Because J_ν and J_ν^{SA} have the same gradient, they differ by a constant, i.e. $J_\nu^{SA} = J_\nu + C$ for some C . But we also know that $J_\nu(\nu) = J(\nu)$, which means that

$$\begin{aligned} C &= J_\nu^{SA}(\nu) - J_\nu(\nu) \\ &= J_\nu^{SA}(\nu) - J(\nu) \\ &= E_{(s,a) \sim \mu^\nu} \left[\left(Q^\nu(s, a) + \frac{c}{1-\gamma} \right) \log \frac{p^\nu(a|s)}{p^\nu(a|s)} \right] \\ &= 0. \end{aligned}$$

Hence, $J_\nu = J_\nu^{SA}$ and, becomes J_ν is a lower bound of J , we have

$$J(\pi) \geq J(\nu) + \sum_s d^\nu(s) \sum_a \left(Q^\nu(s, a) + \frac{c}{1-\gamma} \right) p^\nu(a|s) \log \frac{p^\pi(a|s)}{p^\nu(a|s)}. \quad (18)$$

Setting $\nu = \pi_t$ concludes the proof. \square

Proposition 3 (Improvement guarantees for softmax functional representation). *Assuming that the rewards are in $[0, 1]$, then the surrogate function in Eq. (8) satisfies $J \geq \ell_t^{\pi, \phi, \eta}$ for $\eta \leq 1 - \gamma$.*

Proof. Assume

$$\eta = \frac{1 - \gamma}{r_m - r_l}. \quad (19)$$

We know from Proposition 4 that

$$\ell_t^{z^\pi, \phi, \eta}(\theta) \leq J(\pi_t) + E_{(s,a) \sim \mu^{\pi_t}} \left(A^{\pi_t}(s, a) + \frac{1}{\eta} \right) \log \frac{p^\pi(a|s, \theta)}{p^{\pi_t}(a|s, \theta)} .$$

Since the rewards are between r_l and r_m , we have

$$\begin{aligned} \ell_t^{z^\pi, \phi, \eta}(\pi) &\leq J(\pi_t) + E_{(s,a) \sim \mu^{\pi_t}} \left[\left(A^{\pi_t}(s, a) + \frac{1}{\eta} \right) \log \frac{p^\pi(a|s)}{p^{\pi_t}(a|s)} \right] \\ &= J(\pi_t) + E_{(s,a) \sim \mu^{\pi_t}} \left[\left(A^{\pi_t}(s, a) + \frac{r_m - r_l}{1 - \gamma} \right) \log \frac{p^\pi(a|s)}{p^{\pi_t}(a|s)} \right] \\ &= J(\pi_t) + E_{(s,a) \sim \mu^{\pi_t}} \left[\left(A^{\pi_t}(s, a) + V^{\pi_t}(s) + \left(\frac{r_m}{1 - \gamma} - V^{\pi_t}(s) \right) - \frac{r_l}{1 - \gamma} \right) \log \frac{p^\pi(a|s)}{p^{\pi_t}(a|s)} \right] \\ &= J(\pi_t) + E_{(s,a) \sim \mu^{\pi_t}} \left[\left(Q^{\pi_t}(s, a) - \frac{r_l}{1 - \gamma} \right) \log \frac{p^\pi(a|s)}{p^{\pi_t}(a|s)} \right] \\ &\quad - E_{s \sim d^{\pi_t}} \left[\left(\frac{r_m}{1 - \gamma} - V^{\pi_t}(s) \right) KL(p^{\pi_t}(\cdot|s) \| p^\pi(\cdot|s)) \right] . \end{aligned}$$

The last term on the RHS of the last equation is negative. Indeed, because the rewards are less than r_m , the value functions are less than $r_m/(1 - \gamma)$ and $r_m/(1 - \gamma) - V^{\pi_t}(s)$ is positive. As the KL divergences are positive, the product of the two is positive and the whole term is negative because of the minus term. Thus, we have

$$\begin{aligned} \ell_t^{z^\pi, \phi, \eta}(\pi) &\leq J(\pi_t) + E_{(s,a) \sim \mu^{\pi_t}} \left[\left(Q^{\pi_t}(s, a) - \frac{r_l}{1 - \gamma} \right) \log \frac{p^\pi(a|s)}{p^{\pi_t}(a|s)} \right] \\ &\leq J(\pi) . \end{aligned} \quad (\text{by Lemma 2})$$

Hence, choosing $\eta = \frac{1-\gamma}{r_m-r_l}$ leads to an improvement guarantee. Because our rewards are bounded between 0 and 1, setting $r_m = 1$ and $r_l = 0$ gives $\eta = 1 - \gamma$. This concludes the proof. \square

D Experimental details in the bandit setting

In this section, we detail the experimental setup for the bandit experiments in Section 6.1.

We consider different K -armed Bernoulli bandit problems. For sEXP3, we specialise the update rule in Eq. (8) to this multi-armed bandit case yielding: $p^{\pi_{t+1}}(a) = p^{\pi_t}(a)(1 + \eta A^{\pi_t}(a))$, where η needs to be chosen such that the probabilities are always positive. However, computing the advantage either requires knowledge of the rewards of all arms, or an estimate thereof. Since EXP3 is an adversarial bandit algorithm and does not exploit the stochasticity in the rewards, to ensure a fair comparison, we cannot use such an estimate and thus replace the advantage with the immediate reward, leading to the final sEXP3 update:

$$p^{\pi_{t+1}}(a) = p^{\pi_t}(a)(1 + \eta \hat{r}_t(a)) ,$$

where $\hat{r}_t(a)$ an estimator of the reward $r_t(a)$ obtained at round t .

For sEXP3, if A_t is the action taken at round t , then we use the importance weighted estimator $\hat{r}_t(a) = \mathbb{I}\{A_t = 1\}r_t(a)/\pi_t(a)$. For EXP3, we consider both the standard importance weighted estimator (referred to as IWEXP3 in the plots) and the loss based importance weighted estimator (referred to as LBIWEXP3 in the plots) for which $\hat{r}_t(a) = \mathbb{I}\{A_t = 1\}(1 - r_t(a))/\pi_t(a)$.

Before describing our experimental setup, we emphasize that there are two different sources of randomness in our experiments. First, we have the *environment seed* that controls the mean rewards in the bandit problem. Considering different environment seeds guarantees that our results are not specific to a particular choice of the rewards. Given a specific bandit problem, since EXP3 and sEXP3 are randomized bandit algorithms, there is a stochasticity in the actions chosen. We can use different *agent seeds* to control the algorithm randomness.

Following the evaluation protocol of (Vaswani et al., 2020), we consider two classes of bandits with different action gaps (difference in the mean rewards) – hard instances ($\Delta = 0.5$) and easy instances ($\Delta = 0.1$). The

mean vector defining a Bernoulli bandit is then sampled entry wise (for each arm) from $\mathcal{U}(0.5 - \Delta/2, 0.5 + \Delta/2)$. To obtain the plot in Section 6.1, we run the experiment for 50 different environment seeds and one agent seed. We evaluated the three algorithms for Bernoulli bandits with $K \in \{2, 10, 100\}$ arms and the difficulty of the problem, as determined by the action gap. For each algorithm, we set the step-size via a grid search over $\eta \in \{0.5, 0.05, 0.005, 0.0005, 0.00005\}$. The plot shows the regret corresponding to the step-size with lowest final average regret.

E Additional experiments on MuJoCo environments

In this section, we present results on a series of MuJoCo environments where learning rate decay and gradient clipping have *not* been applied. Fig. 3 shows that, while sPPO (in orange) still learns something, PPO is unable to make progress, regardless of the capping (ϵ) and the number of inner loop steps (m), further reinforcing our intuition that the softmax parameterization leads to a more robust optimization.

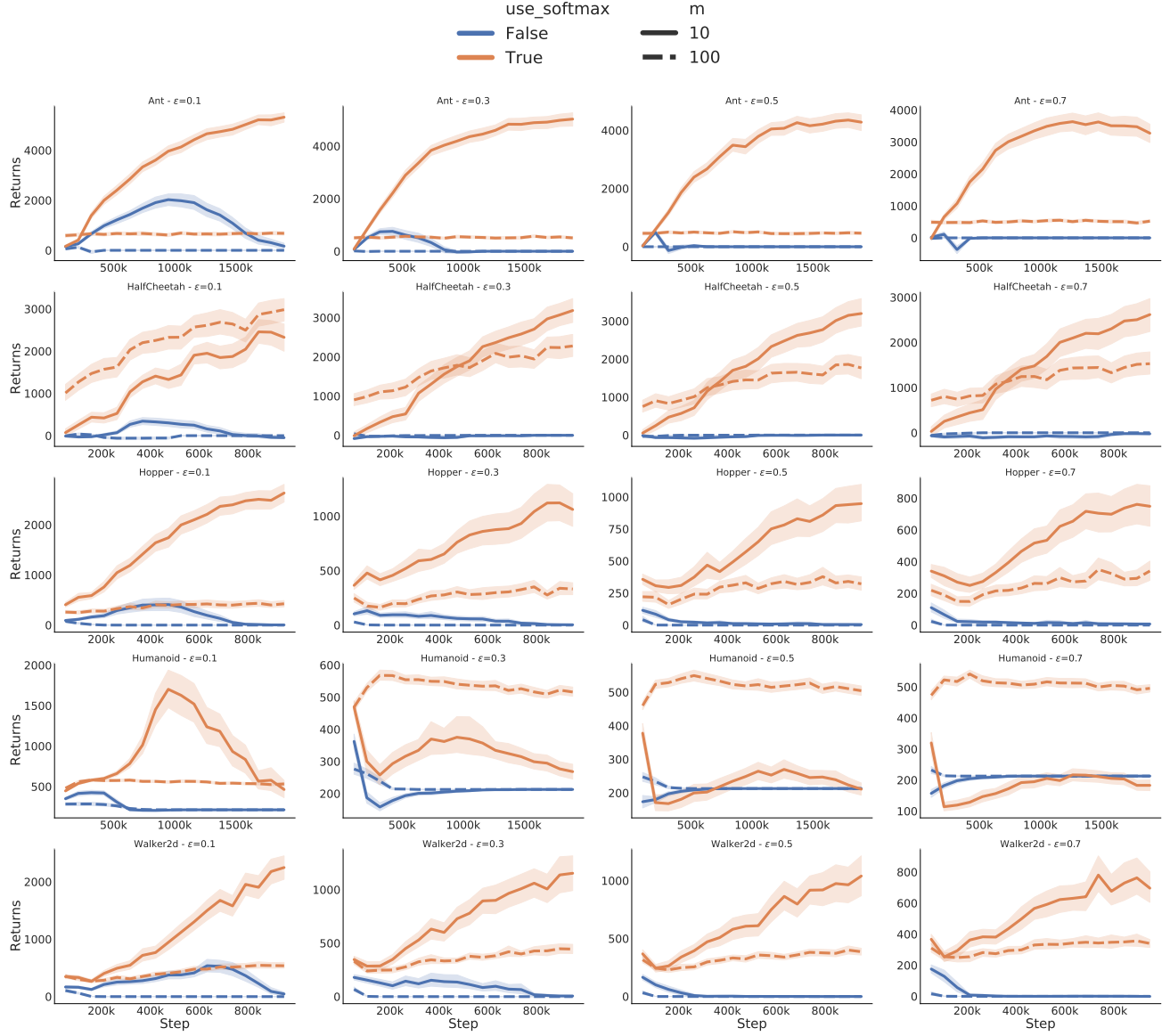


Figure 3: Average discounted return and 95% confidence interval (over 180 runs) for PPO and softmax PPO on 4 environments (*env* - rows) and for four different clipping strengths (*epsilon* - columns). We see that sPPO is more robust to large values of clipping, even more so when the number of updates in the inner loop grows (linestyle).